Eur. Phys. J. Appl. Phys. **32**, 199–206 (2005)
DOI: 10.1051/epjap:2005091

THE EUROPEAN PHYSICAL JOURNAL
APPLIED PHYSICS

Guided ultrasonic waves in the cylindrical layer-substrate structures. Application to the control of the massive machine elements with cylindrical cavities

M. El Ouahdani[1], M. Sidki[a], and A. Ramdani

Laboratory of control and characterization of materials, Department of Physics, Faculty of Sciences, BP 20, 24000 El Jadida, Morocco

Received: 28 February 2005 / Received in final form: 4 June 2005 / Accepted: 20 July 2005
Published online: 14 December 2005 – © EDP Sciences

Abstract. This paper presents a study of the ultrasonic wave propagation in a cylindrical layer-substrate structure of an infinite length. We determine the dispersion curves of the structure, the displacements field in the structure and the impact of the contact quality between the layer and the substrate. The industrial application aimed by our study is the control of the massive machine elements with cylindrical cavities coated and exposed to corrosion. The obtained results show that some modes of propagation are insensitive to the layer thickness. Therefore, these modes can be generated during the ultrasonic control of the layer. In addition, for the dimensions considered here, the second mode of propagation is the most adapted for the detection of defects in the vicinity of the internal layer wall. In addition, our study shows the possibility of characterization of the quality of contact between the layer and the substrate from the analysis of dispersion curves of the structure.

PACS. 68.60.Bs Mechanical and acoustical properties – 43.20.Mv Waveguides, wave propagation in tubes and ducts

1 Introduction

The non destructive ultrasonic control of cylindrical machine elements is of a great importance in car, plane and space industries. It contributes to a substantial cost reduction of these elements production.

The use of ultrasounds as mean of control requires the study and the understanding of the ultrasonic guided waves propagation in cylindrical structures. Many contributions on this subject can be found in the scientific literature.

Viktorov [1,2] and Ruff [3] studied the ultrasonic propagation on a cylindrical surface to detect surface defects. Mindlin [4] deals with the ultrasonic propagation in the axial direction of a cylindrical rods. Gazis [5] and Rose et al. [6] studied the guided ultrasonic propagation in hollow cylinders. Qu et al. [7] and Liu and Qu [8] examined the propagation of ultrasonic waves in cylindrical annulus. Epstein [9] studied the ultrasonic propagation in a composite circular cylinder. He examined the variation of the phase velocity for the first propagation modes for bonded and smooth contact conditions. Valle et al. [10] numerically solved the dispersion relation for the case of a layered cylinders with an interface of smooth contact.

Our work deals with the case of a cylindrical layer/substrate structure with boundary conditions on the inner wall of the layer and on the interface layer-substrate. We developed a program on Matlab to determine dispersion curves and displacements fields in the structure aiming to determine the most adapted propagation modes for the structure control. Furthermore, a mathematical modelling of the contact layer-substrate permitted us to examine the impact of the quality of this contact on dispersion curves of the structure. The industrial application aimed by our study is the control of the massive machine elements with cylindrical cavities like cylindrical coated holes used for distribution or injection of air, oil, or fuel in car and aircraft industries. These holes are exposed to corrosion and crack fatigue and need to be controlled.

[a] e-mail: sidkimouncif@hotmail.com

2 Problem position

The studied system is a cylindrical layer/substrate structure of an infinite length (Fig. 1). The layer is in chromium and the substrate is in steel.

The propagation equation in a linearly elastic and isotropic solid is given by [11,12]

$$\rho\frac{\partial^2\vec{u}}{\partial t^2} = (\lambda+2\mu)\mathrm{gr\vec{a}d}(\mathrm{div}\vec{u}) - \mu.\mathrm{r\vec{o}t}(\mathrm{r\vec{o}t}\vec{u}) \quad (1)$$

where $\vec{u}$ is the displacement vector, λ, μ are the Lamé constants and ρ is the solid density. The displacement $\vec{u}$

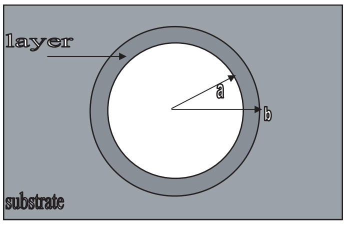

Fig. 1. Cylindrical layer/substrate structure.

can be written as:

$$\vec{u} = \vec{\mathrm{grad}}\phi + \vec{\mathrm{rot}}\vec{\psi} \tag{2}$$

ϕ *is a* scalar potential and $\vec{\psi}$ *is a* vector potential.

Substituting this expression of $\vec{u}$ in equation (1), we obtain:

$$\Delta\phi = \frac{1}{c_l^2}.\frac{\partial^2\phi}{\partial t^2} \tag{3}$$

$$\Delta\vec{\psi} = \frac{1}{c_t^2}.\frac{\partial^2\vec{\psi}}{\partial t^2} \tag{4}$$

$$\text{where} \quad c_l = \sqrt{\frac{\lambda+2\mu}{\rho}}, \quad c_t = \sqrt{\frac{\mu}{\rho}} \tag{5}$$

c_l and c_t are the longitudinal and shear wave velocities in the solid.

The general solutions of equations (3, 4) in cylindrical coordinates (r, θ) are given by:

– for the layer:

$$\varphi(r,\theta,t) = [AJ_n(\alpha_1 kr) + BY_n(\alpha_1 kr)]\exp(-iwt)\sin(n\theta) \tag{6}$$

$$\psi_z(r,\theta,t) = [CJ_n(\beta_1 kr) + DY_n(\beta_1 kr)]\exp(-iwt)\cos(n\theta) \tag{7}$$

– for the substrate:

$$\varphi(r,\theta,t) = EH_n^{(1)}(\alpha kr)\exp(-iwt)\sin(m\theta) \tag{8}$$

$$\psi_z(r,\theta,t) = FH_n^{(1)}(\beta kr)\exp(-iwt)\cos(m\theta) \tag{9}$$

where: $k = \frac{w}{c}$, $\alpha_1 = \frac{c}{c_{l1}}$, $\beta_1 = \frac{c}{c_{t1}}$, $\alpha = \frac{c}{c_l}$, $\beta = \frac{c}{c_t}$, w denotes the angular frequency, c_l and c_t are the longitudinal and shear wave velocities in the substrate, c_{l1} and c_{t1} are the longitudinal and shear wave velocities in the layer, c is the velocity of circumferential modes (the index 1 is related to the layer), $J_n(x), Y_n(x)$ denotes Bessel functions of the first and second kind, $H_n^{(1)}(x)$ denotes Hankel function of the first kind, *A, B, C, D, E, F* are constants.

The displacements, u_r and u_θ, and the stresses, σ_{rr} and $\sigma_{r\theta}$ are derived from potentials according to the following equations:

$$u_r = \frac{\partial\varphi}{\partial r} + \frac{1}{r}\frac{\partial\psi_z}{\partial\theta} \tag{10}$$

$$u_\theta = \frac{1}{r}\frac{\partial\varphi}{\partial\theta} - \frac{1}{r}\frac{\partial\psi_z}{\partial r} \tag{11}$$

$$\sigma_{rr} = \lambda\left(\frac{\partial u_r}{\partial r} + \frac{u_r}{r} + \frac{1}{r}\frac{\partial u_\theta}{\partial\theta}\right) + 2\mu\frac{\partial u_r}{\partial r} \tag{12}$$

$$\sigma_{r\theta} = \mu\left(\frac{\partial u_\theta}{\partial r} - \frac{u_\theta}{r} + \frac{1}{r}\frac{\partial u_r}{\partial\theta}\right). \tag{13}$$

For the studied system, the boundary conditions are:

2.1 Perfect layer – substrate contact

$r = a$; (free boundary):

$$\sigma_{rr}^{(1)}(a,\theta,t) = \sigma_{r\theta}^{(1)}(a,\theta,t) = 0 \tag{14}$$

$r = b$; (continuity of displacements and stresses):

$$u_r^{(1)}(b,\theta,t) = u_r(b,\theta,t) \tag{15}$$

$$u_\theta^{(1)}(b,\theta,t) = u_\theta(b,\theta,t) \tag{16}$$

$$\sigma_{rr}^{(1)}(b,\theta,t) = \sigma_{rr}(b,\theta,t) \tag{17}$$

$$\sigma_{r\theta}^{(1)}(b,\theta,t) = \sigma_{r\theta}(b,\theta,t) \tag{18}$$

Exponent $^{(1)}$ is attributed to the layer.

These boundary conditions lead to the following equations: $n = m = kb$ (the angular wave numbers n and m must be equal at the interface), $[M]X = 0$, where $X = [A,B,C,D,E,F]^T$. The 6×6 matrix $[M]$ is presented in Appendix A.

For non-trivial solutions X, we must have Det $[M] = 0$: the dispersion relation for the circumferential modes.

The determinant is function of the frequency of excitation f and the phase velocity c of modes. The solutions of the dispersion relation are couples (f,c) for which the determinant is nul, i.e. det $[M] = 0$. These roots were calculated for a selected range of frequencies using the bisection method. Once the dispersion relation solved, the components of the vector X are determined. Substituting these values in the expression of potentials and then in the displacements, we derive the vector displacement of the circumferential wave:

$$u_r^{(1)}(r,\theta,t) = U_r^{(1)}(r)\exp(-iwt)\sin(n\theta) \tag{19}$$

$$u_\theta^{(1)}(r,\theta,t) = U_\theta^{(1)}(r)\exp(-iwt)\cos(n\theta) \tag{20}$$

$$u_r(r,\theta,t) = U_r(r)\exp(-iwt)\sin(m\theta) \tag{21}$$

$$u_\theta(r,\theta,t) = U_\theta(r)\exp(-iwt)\cos(m\theta) \tag{22}$$

$$U(r) = W(r).X \tag{23}$$

where: $U(r) = (U_r^{(1)}, U_\theta^{(1)}, U_r, U_\theta)_T$ and W is matrix whose elements are given in Appendix B.

2.2 Imperfect contact – Pilarski model

To study the impact of the contact (layer/substrate) on the dispersion curves, the interface continuity conditions considered in the previous paragraph are replaced by those defined by Pilarski [13].

– Continuity of the stresses at each interface:

$$\sigma_{r\theta}^{(1)}(b,\theta,t) = \sigma_{r\theta}(b,\theta,t) \tag{24}$$

$$\sigma_{rr}^{(1)}(b,\theta,t) = \sigma_{rr}(b,\theta,t). \tag{25}$$

– Proportionality relation between the stresses and the difference of the displacement components at each interface:

$$\sigma_{r\theta}^{(1)} = K_t \left(u_\theta^{(1)} - u_\theta\right) \quad (26)$$

$$\sigma_{rr}^{(1)} = K_n \left(u_r^{(1)} - u_r\right) \quad (27)$$

K_n and K_t are the parameters which characterize the interfaces. They are expressed in $\mathrm{N\,m^{-3}}$.

The writing of the above proportionality relations in the form $U_{\theta,r}^{(1)} = U_{\theta,r}^{+} \frac{\sigma_{r\theta,r}^{(1)}}{K_{t,n}}$ shows that when we give the parameter $K_{t,n}$ a very large value the term $\frac{\sigma_{r\theta,r}^{(1)}}{K_{t,n}}$ tends towards zero which gives the equality of the displacement components on the both sides of the interfaces. It is the perfect contact case.

3 Numerical results and discussion

The physical properties of the chromium layer and the steel substrate are:

- $\rho_1 = 7194$ Kg/m^3, c_{l1}=6608 m/s, $c_{t1} = 4005$ m/s
- $\rho = 7800$ Kg/m^3, $c_l = 5980$ m/s, $c_t = 3297$ m/s.

The inner radius of layer is $a = 0.3$ cm.

We define the following non-dimensional parameters:
h/b; h is the layer thickness; b is the outer radius of the layer,
c/c_{t1}; c velocity of the circumferential wave,
$\Omega = \omega.b/c_t$: normalized frequency,
$r_i = (r - a)/h$; r radial distance.

Figure 2 presents the dispersion curves ((c/c_{t1}) versus Ω) of the layer/substrate structure for different values of h/b. We note that, except the first mode, all circumferential modes preserve their shapes. These modes, insensitive to the thickness, can therefore be selected for ultrasonic inspection of the layer. Table 1 giving velocities of the modes for three normalized frequencies, illustrates this observation.

Radial and tangential displacements of circumferential modes are calculated for the normalised frequency $\Omega = 94.04$, corresponding to an excitation frequency of 15 MHz. The values of c/c_{t1} corresponding to the first six modes are:

$c/c_{t1} = 0.895$; 1.054; 1.113; 1.165; 1.215; 1.265.

Figure 3 presents the distribution of radial and tangential displacements in the layer as a function of r_i. For the second mode (Fig. 3b), the major part of the energy is concentrated in the inner surface of the layer. Therefore, this mode is the most adapted for the detection of the corrosion on the inner surface.

The perfect contact of the studied system, is obtained when we give parameters K_n and K_t the value of 10^{15} $\mathrm{N\,m^{-3}}$. Figure 4a presents the dispersion curves determined numerically in the case of a perfect contact. The decrease of the contact quality between the layer and the substrate is simulated by giving parameters K_n and K values lower than 10^{15} $\mathrm{N\,m^3}$. The dispersion curves as function of the contact quality, are presented in Figures 4b–d. As the contact quality decreases i.e. decreasing of the values of K_n and K_t, new propagation modes appear. We note clearly that for values of order of 10^{10}, we find dispersion curves similar to those of the layer (Fig. 5). These values of K_n and K_t simulate the case of an almost complete disbonding of the layer.

4 Conclusion

The research work presented here, permitted to study and understand the propagation of circumferential waves in a cylindrical layer-substrate structure. We solved numerically, the dispersion relation. We determine the dispersion curves and the displacements field in the structure. Applied to the massive machine elements with cylindrical cavities, this work permitted to identify the most adapted modes for the ultrasonic control of the layer (defects detection). The most adapted modes for the inspection of the inner surface of the layer (corrosion detection) have been identified also.

Furthermore, we showed the possibility of characterization of the contact quality (from perfect contact to the complete disbonding) between the layer and the substrate from the dispersion curves of the structure.

Appendix A

The elements of the matrix M_{ij} are:

$$M(1,1) = \left(2 + \frac{2}{n} - \frac{\beta_1^2}{g^2}\right) JA_{1aa0} - \frac{2\alpha_1}{gn} JA_{1a};$$

$$M(1,2) = \left(2 + \frac{2}{n} - \frac{\beta_1^2}{g^2}\right) YA_{1aa0} - \frac{2\alpha_1}{gn} YA_{1a}; \quad (A.1)$$

$$M(1,3) = 2\left(\frac{\beta_1}{g} JB_{1a} - \left(1 + \frac{1}{n}\right) JB_{1a0}\right);$$

$$M(1,4) = 2\left(\frac{\beta_1}{g} YB_{1a} - \left(1 + \frac{1}{n}\right) YB_{1a0}\right); \quad (A.2)$$

$$M(1,5) = 0; M(1,6) = 0. \quad (A.3)$$

$$M(2,1) = 2\left(\frac{\alpha_1}{g} JA_{1a} - \left(1 + \frac{1}{n}\right) JA_{1a0}\right);$$

$$M(2,2) = 2\left(\frac{\alpha_1}{g} YA_{1a} - \left(1 + \frac{1}{n}\right) YA_{1a0}\right). \quad (A.4)$$

$$M(2,3) = \left(2 + \frac{2}{n} - \frac{\beta_1^2}{g^2}\right) JB_{1aa0} - \frac{2\beta_1}{gn} JB_{1a};$$

$$M(2,4) = \left(2 + \frac{2}{n} - \frac{\beta_1^2}{g^2}\right) YB_{1aa0} - \frac{2\beta_1}{gn} YB_{1a}. \quad (A.5)$$

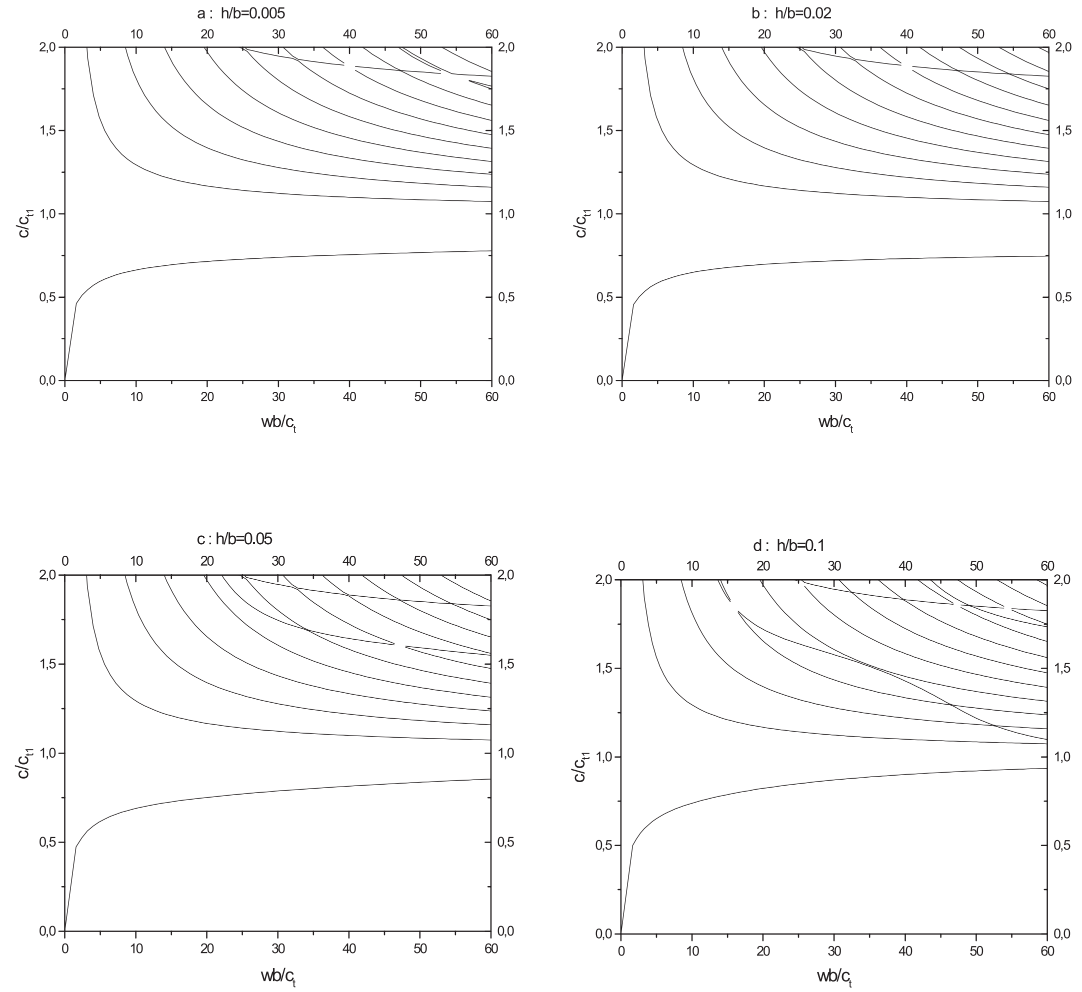

Fig. 2. Dispersion curves of the system chromium/steel. Perfect contact **a**: $h/b = 0.005$; **b**: $h/b = 0.02$; **c**: $h/b = 0.05$; **d**: $h/b = 0.1$.

Table 1. Velocities of modes for the normalized frequencies 10, 30, 60, for different thickness.

Ω	h/b	c/c_{t1}															
10	0.005	0.64	1.29	1.81													
	0.02	0.66	1.29	1.81													
	0.05	0.68	1.29	1.81													
	0.1	0.73	1.29	1.81													
30	0.005	0.71	1.12	1.27	1.43		1.60		1.80	1.94							
	0.02	0.73	1.12	1.27	1.43		1.60		1.80	1.94							
	0.05	0.78	1.12	1.27	1.43		1.60	1.74	1.80	1.94							
	0.1	0.86	1.12	1.27	1.43	1.57	1.60		1.80	1.94							
60	0.005	0.74	1.07		1.15	1.23	1.31	1.39	1.47		1.56	1.65		1.74		1.82	1.85
	0.02	0.77	1.07		1.15	1.23	1.31	1.39	1.47		1.56	1.65		1.74	1.76	1.82	1.85
	0.05	0.85	1.07		1.15	1.23	1.31	1.39	1.47	1.54	1.56	1.65		1.74		1.82	1.85
	0.1	0.93	1.07	1.09	1.15	1.23	1.31	1.39	1.47		1.56	1.65	1.73	1.74		1.82	1.85

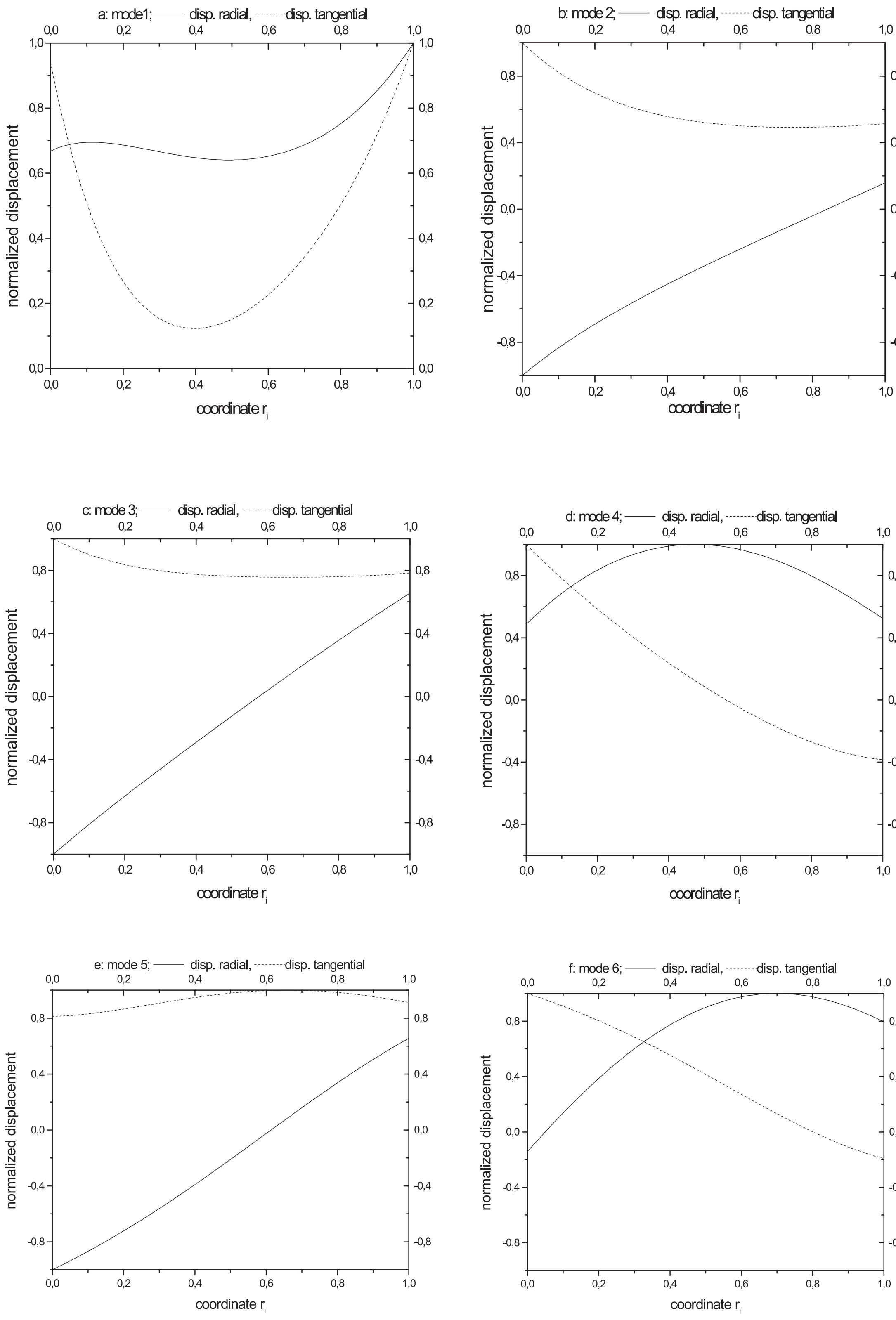

Fig. 3. Normalized radial and tangential displacements distribution along the radial direction, in the layer for a frequency of 15 MHz (for the first six modes), **a**: mode 1; **b**: mode 2; **c**: mode 3; **d**: mode 4 ; **e**: mode 5; **f**: mode 6.

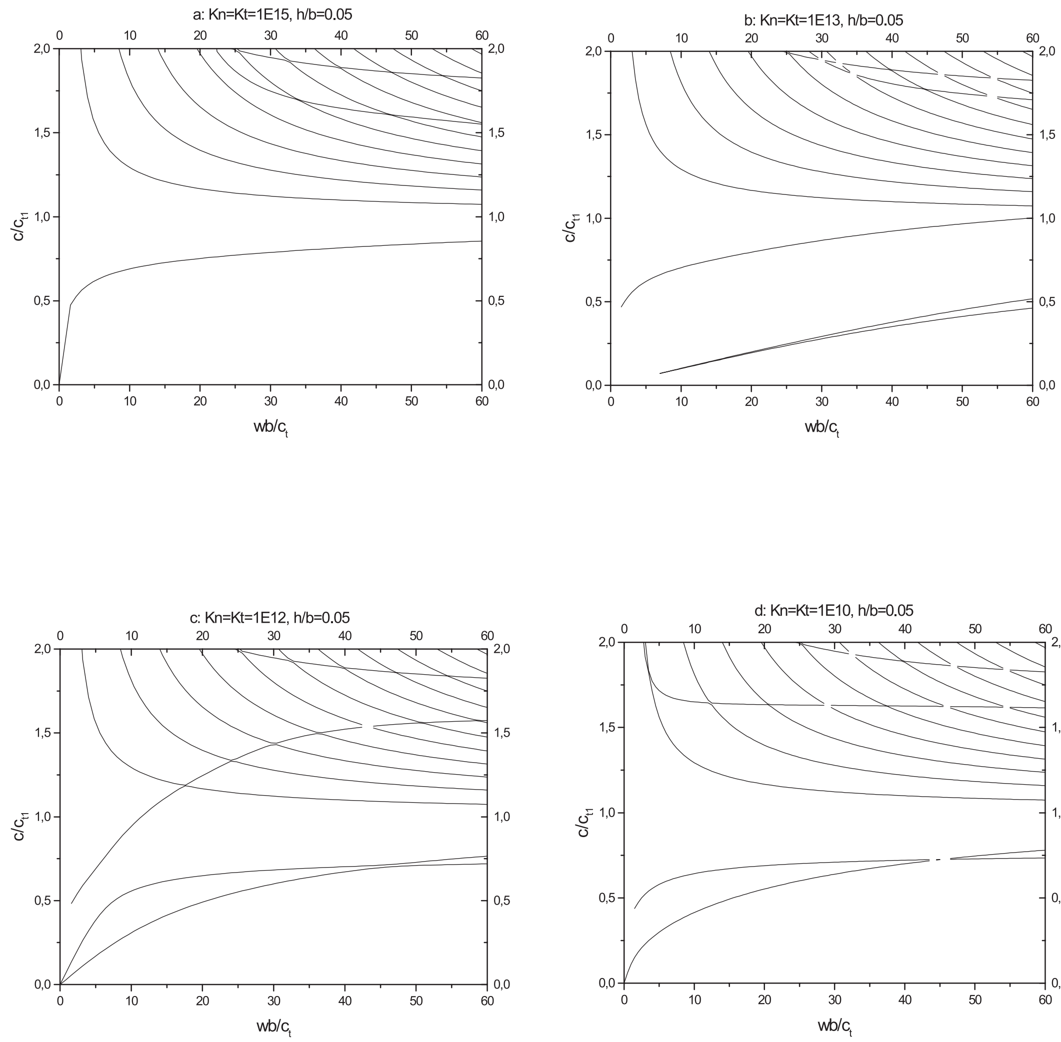

Fig. 4. Dispersion curves of the system chromium/steel. Imperfect contact **a**: $K_n = K_t = 1\text{E}15$, $h/b = 0.05$; **b**: $K_n = K_t = 1\text{E}13$, $h/b = 0.05$; **c**: $K_n = K_t = 1\text{E}12$, $h/b = 0.05$; **d**: $K_n = K_t = 1\text{E}10$, $h/b = 0.05$.

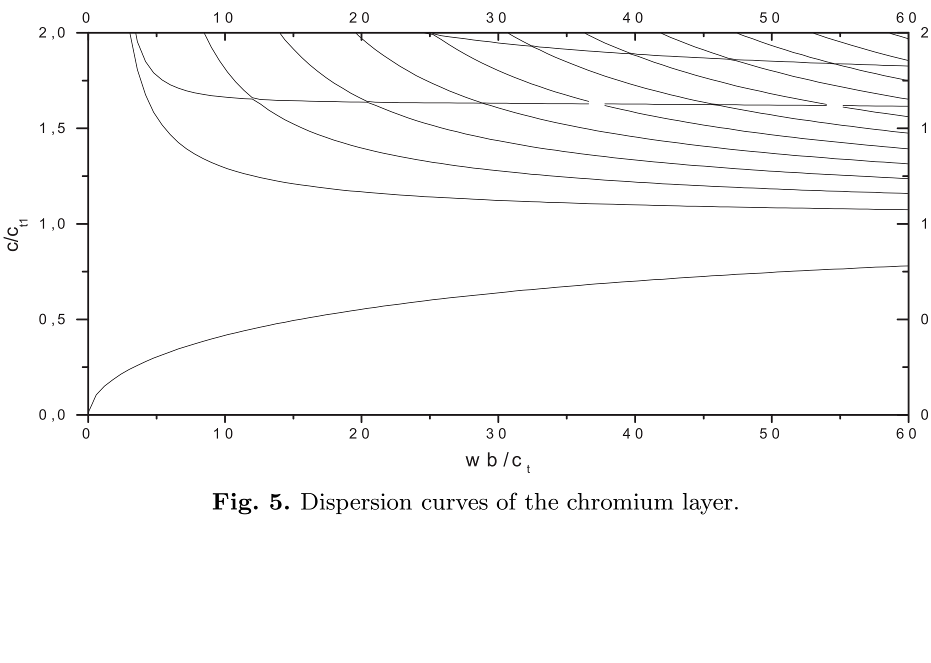

Fig. 5. Dispersion curves of the chromium layer.

$$M(2,5) = 0; M(2,6) = 0. \tag{A.6}$$

$$M(3,1) = \gamma\left[2 - \beta_1^2 - \frac{2}{n}(\alpha_1 JA_1 - 1)\right]; \quad M(3,2) = \gamma\left[2 - \beta_1^2 - \frac{2}{n}(\alpha_1 YA_1 - 1)\right]. \tag{A.7}$$

$$M(3,3) = 2\gamma\left(\beta_1 JB_1 - 1 - \frac{1}{n}\right); \quad M(3,4) = 2\gamma\left(\beta_1 YB_1 - 1 - \frac{1}{n}\right). \tag{A.8}$$

$$M(3,5) = 2 - \beta^2 - \frac{2}{n}\left(\alpha HA_1 - 1\right); \quad M(3,6) = 2\left(\beta HB_1 - 1 - \frac{1}{n}\right). \tag{A.9}$$

$$M(4,1) = 2\gamma\left(\alpha_1 JA_1 - 1 - \frac{1}{n}\right); \quad M(4,2) = 2\gamma\left(\alpha_1 YA_1 - 1 - \frac{1}{n}\right). \tag{A.10}$$

$$M(4,3) = \gamma\left[2 - \beta_1^2 - \frac{2}{n}(\beta_1 JB_1 - 1)\right]; \quad M(4,4) = \gamma\left[2 - \beta_1^2 - \frac{2}{n}(\beta_1 YB_1 - 1)\right]. \tag{A.11}$$

$$M(4,5) = -2\left(1 + \frac{1}{n} - \alpha HA_1\right); \quad M(4,6) = -\left[\beta^2 - 2 + \frac{2}{n}(\beta HB_1 - 1)\right]. \tag{A.12}$$

$$M(5,1) = \alpha_1 JA_1 - 1; M(5,2) = \alpha_1 YA_1 - 1; M(5,3) = 1; \quad M(5,5) = \alpha HA_1 - 1; M(5,6) = 1. \tag{A.13}$$

$$M(6,1) = 1; M(6,2) = 1; M(6,3) = \beta_1 JB_1 - 1. \tag{A.14}$$

$$M(6,4) = \beta_1 YB_1 - 1; M(6,5) = 1; M(6,6) = \beta HB_1 - 1. \tag{A.15}$$

$$\gamma = \frac{\mu_1}{\mu}, \quad g = \frac{b}{a}, \quad \alpha_1 = \frac{c}{c_{l1}}, \quad \beta_1 = \frac{c}{c_{t1}}, \quad \alpha = \frac{c}{c_l}, \quad \beta = \frac{c}{c_t}, \quad k = \frac{w}{c}, \quad h = b - a. \tag{A.16}$$

λ_1 and μ_1 are the Lamé constants of the layer; λ and μ are the Lamé constants of the substrate.

$$HA_1 = \frac{H_{n-1}^{(1)}(\alpha kb)}{H_n^{(1)}(\alpha kb)}; HB_1 = \frac{H_{n-1}^{(1)}(\beta kb)}{H_n^{(1)}(\beta kb)}. \tag{A.17}$$

$$JA_1 = \frac{J_{n-1}(\alpha_1 kb)}{J_n(\alpha_1 kb)} \quad JB_1 = \frac{J_{n-1}(\beta_1 kb)}{J_n(\beta_1 kb)} \quad JA_{1a} = \frac{J_{n-1}(\alpha_1 ka)}{J_n(\alpha_1 kb)} \tag{A.18}$$

$$JB_{1a} = \frac{J_{n-1}(\beta_1 ka)}{J_n(\beta_1 kb)} \quad JA_{1a0} = \frac{J_n(\alpha_1 ka)}{J_n(\alpha_1 kb)} \quad JB_{1a0} = \frac{J_n(\beta_1 ka)}{J_n(\beta_1 kb)} \tag{A.19}$$

$$YA_1 = \frac{Y_{n-1}(\alpha_1 kb)}{Y_n(\alpha_1 kb)} \quad YB_1 = \frac{Y_{n-1}(\beta_1 kb)}{Y_n(\beta_1 kb)} \tag{A.20}$$

$$YA_{1a} = \frac{Y_{n-1}(\alpha_1 ka)}{Y_n(\alpha_1 kb)} \quad YB_{1a} = \frac{Y_{n-1}(\beta_1 ka)}{Y_n(\beta_1 kb)} \quad YA_{1a0} = \frac{Y_n(\alpha_1 ka)}{Y_n(\alpha_1 kb)} \quad YB_{1a0} = \frac{Y_n(\beta_1 ka)}{Y_n(\beta_1 kb)}. \tag{A.21}$$

Appendix B

The elements of the matrix W_{ij} are:

$$W(1,1) = \alpha_1 JA_1 - \frac{b}{r} JA_0; W(1,2) = \alpha_1 YA_1 - \frac{b}{r} YA_0; \quad W(1,3) = \frac{b}{r} JB_0. \tag{B.1}$$

$$W(1,4) = \frac{b}{r} YB_0; W(1,5) = W(1,6) = 0. \tag{B.2}$$

$$W(2,1) = \frac{b}{r} JA_0; W(2,2) = \frac{b}{r} YA_0; \quad W(2,3) = \beta_1 JB_1 - \frac{b}{r} JB_0. \tag{B.3}$$

$$W(2,4) = \beta_1 YB_1 - \frac{b}{r} YB_0; W(2,5) = W(2,6) = W(3,1) = W(3,2) = W(3,3) = W(3,4) = 0. \tag{B.4}$$

$$W(3,5) = \frac{b}{r} HA_0 - \alpha HA_1; W(3,6) = -\frac{b}{r} HB_0. \tag{B.5}$$

$$W(4,1) = W(4,2) = W(4,3) = W(4,4) = 0; \quad W(4,5) = -\frac{b}{r} HA_0; W(4,6) = \frac{b}{r} HB_0 - \beta HB_1. \tag{B.6}$$

$$HA_1 = \frac{H^{(1)}_{n-1}(\alpha kr)}{H^{(1)}_n(\alpha n)}$$

$$HB_1 = \frac{H^{(1)}_{n-1}(\beta kr)}{H^{(1)}_n(\beta n)} \quad HA_0 = \frac{H^{(1)}_n(\alpha kr)}{H^{(1)}_n(\alpha n)} \tag{B.7}$$

$$HB_0 = \frac{H^{(1)}_n(\beta kr)}{H^{(1)}_n(\beta n)}$$

$$JA_1 = \frac{J_{n-1}(\alpha_1 kr)}{J_n(\alpha_1 n)} \quad JA_0 = \frac{J_n(\alpha_1 kr)}{J_n(\alpha_1 n)} \tag{B.8}$$

$$YA_1 = \frac{Y_{n-1}(\alpha_1 kr)}{Y_n(\alpha_1 n)} \quad YA_0 = \frac{Y_n(\alpha_1 kr)}{Y_n(\alpha_1 n)} \tag{B.9}$$

$$JB_1 = \frac{J_{n-1}(\beta_1 kr)}{J_n(\beta_1 n)} \quad JB_0 = \frac{J_n(\beta_1 kr)}{J_n(\beta_1 n)}$$

$$YB_1 = \frac{Y_{n-1}(\beta_1 kr)}{Y_n(\beta_1 n)} \quad YB_0 = \frac{Y_n(\beta_1 kr)}{Y_n(\beta_1 n)} \tag{B.10}$$

References

1. I.A. Victorov, Acoust. Appl. Mech. **65**, 424 (1958)
2. I.A. Victorov, *Rayleigh and Lamb Waves* (Plenum, New York, 1967)
3. B. Ruff, J. Acoust. Soc. Am. **45**, 493 (1969)
4. R.D. Mindlin, J. Appl. Mech. **82**, 145 (1960)
5. D.I. Gazis, J. Acoust. Soc. Am. **31-35**, 568 (1959)
6. J.L. Rose, J.J. Ditri, A. Pilarski, K. Rajana, F. Carr, NDT E Int. **27**, 307 (1994)
7. J. Qu, Y. Berthelot, Z. Li, Rev. Prog. Quant. NDE **15A**, 169 (1996)
8. G. Liu, J. Qu, J. Appl. Mech. **65**, 424 (1998)
9. H.L. Epstein, J. Sound Vib. **48**, 57 (1976)
10. C. Valle, J. Qu, L.J. Jacobs, Int. J. Eng. Sci. **37**, 1369 (1999)
11. L.M. Brekhovskikh, *Waves in layered media*, 2nd edn. (Academic Press, New York, 1980)
12. E. Dieulesaint, D. Royer, *Ondes élastiques dans les solides–Application au traitement du signal* (Masson, Paris, 1974)
13. A. Pilarski, J.L. Rose, J. Appl. Phys. **63**, 300 (1988)